



Science Arts & Métiers (SAM)

is an open access repository that collects the work of Arts et Métiers Institute of Technology researchers and makes it freely available over the web where possible.

This is an author-deposited version published in: <https://sam.ensam.eu>
Handle ID: <http://hdl.handle.net/10985/11656>

To cite this version :

Esteve ERNAULT, Bruno FAYOLLE, Emmanuel RICHAUD - Thermal-oxidation of epoxy/amine followed by glass transition temperature changes - Polymer Degradation and Stability - Vol. 138, p.82-90 - 2017

Any correspondence concerning this service should be sent to the repository

Administrator : scienceouverte@ensam.eu



Thermal-oxidation of epoxy/amine followed by glass transition temperature changes

Esteve Ernault, Emmanuel Richaud*, Bruno Fayolle

PIMM UMR 8006, Arts et Métiers ParisTech, CNRS, CNAM, 151 bd de l'Hôpital, Paris, France

ARTICLE INFO

Article history:

Received 23 January 2017

Received in revised form

22 February 2017

Accepted 26 February 2017

Available online 28 February 2017

Keywords:

Epoxy/diamine

Glass transition

Chain scission

Crosslinking

ABSTRACT

Thermal oxidation of three epoxy resins differing by the nature of prepolymer (bisphenol A diglycidyl ether and 1,4-butanediol diglycidyl ether) and hardener (isophorone diamine and 4,7,10-Trioxa-1,13-tridecanediamine) was studied by monitoring changes in glass transition temperature using DSC. Results were discussed using the DiMarzio's approach in which parameters are estimated from an additive group contribution. This theory allowed a fair assessment of T_g values for unaged networks. During oxidation, epoxy networks were shown to undergo chain scissions occurring in great part in hydroxypropyl ether and isophorone groups. However, the exploitation of T_g changes showed the coexistence and even the predominance of crosslinking in materials having linear aliphatic segments. The DiMarzio's approach was used to discuss the possibility of intramolecular cyclization or intermolecular crosslinks which were shown to predominate. Crosslinks were tentatively justified from a mechanistic point of view and quantified depending on experimental conditions.

1. Introduction

Since they are designed for high temperatures applications as matrix for composites, most of the epoxy networks are made of a rigid epoxy and rigid hardener (for example DGEBA/DDS or DGEBA/DDM) [1–13]. Their degradation is very often studied by mass loss [4,6,8,10] which is clearly shown:

- to be associated to the chain scission induced by decomposition of hydroperoxides [7,8].
- to occur quasi instantaneously, since hydroperoxides formed in epoxy amine networks are unstable due to the vicinity of heteroatoms (see for example Table 4.15 vs Table 7.15 in Ref. [14]) which induces the short kinetic chains being an intrinsic characteristic of epoxy resins [8].

It is thus not surprising that mass losses exceeding 10% are measured during thermal ageing [4,6,8] which leads to shrinkage in the oxidized superficial layer in the case of thick samples [15,16].

Some studies also address the consequences of oxidation on the architecture of polymer networks. They show the depletion of glass

transition i.e. that rigid networks (with T_g higher than 150 °C) undergo chain scissions [1,11,13,17].

This short literature review suggests the existence of a major or even exclusive chain scission process leading to the loss of mass and ultimate mechanical properties. However, those phenomena were mainly evidenced in rigid epoxy/diamine systems where 2-hydroxypropyl ether is possibly the only reactive site. The case of flexible epoxies ($T_g < 100$ °C) [18,19] was more scarcely studied so that we were interested in investigating:

- if the above scenario is common to all epoxy networks, or if there are some peculiarities for epoxies with aliphatic linear groups.
- if chain scissions exclusively occur or could they be counter-balanced by crosslinking events ?
- if there is an influence of external parameters (temperature, oxygen pressure) on the consequences of oxidation (at molecular scale i.e. the consequences of the formation of carbonyls or amides), and on the architecture of epoxy networks and later on its thermomechanical properties.

To answer those questions, our investigations will base on a series of epoxy/amine networks differing by their content in aliphatic sequences [20]. Their thermal degradation will be studied at several temperatures and oxygen pressures. A modeling

* Corresponding author.

E-mail address: emmanuel.richaud@ensam.eu (E. Richaud).

approach based on DiMarzio's equation [21] will be first checked on unaged networks and then adapted for taking into account the presence of chain scissions and crosslinks. It will be used to quantify the changes at macromolecular level.

2. Experimental

2.1. Materials

Epoxy/diamine systems were synthesized using the resins and hardeners shown in Fig. 1:

- A Diglycidyl ether of bisphenol A DER 332 resin named here DGEBA (CAS 1675-54-3 – ref 31185 supplied by Sigma Aldrich) has a degree of polymerization n close to 0 and a number average molecular mass equal to 340 g mol^{-1} .
- A Diglycidyl ether of 1,4-butanediol resin named here DGEBU (CAS 2425-79-8 ref 220892 supplied by Sigma Aldrich, $M = 202.25 \text{ g mol}^{-1}$).
- An isophorone diamine hardener named here IPDA (CAS 2855-13-2 – ref 118184 supplied by Sigma Aldrich, $M = 170.3 \text{ g mol}^{-1}$).
- A 4,7,10-Trioxa-1,13-tridecanediamine hardener named here TTDA (CAS 4246-51-9 – ref 369519 supplied by Sigma Aldrich, $M = 220.3 \text{ g mol}^{-1}$).

By combining those resins and hardeners, three systems were chosen: DGEBA/IPDA, DGEBA/TTDA, DGEBU/IPDA. These components were mixed in stoichiometric ratio and fully cured as checked by DSC from the total disappearance of exothermal signal and by FTIR from the total disappearance of epoxide peak at 914 cm^{-1} . Curing enthalpies, curing cycles, final glass transition temperatures are listed in Table 1. In order to avoid the so-called Diffusion Limited Oxidation, films thinner than $100 \mu\text{m}$ were made using a heating press (Gibrite Instruments).

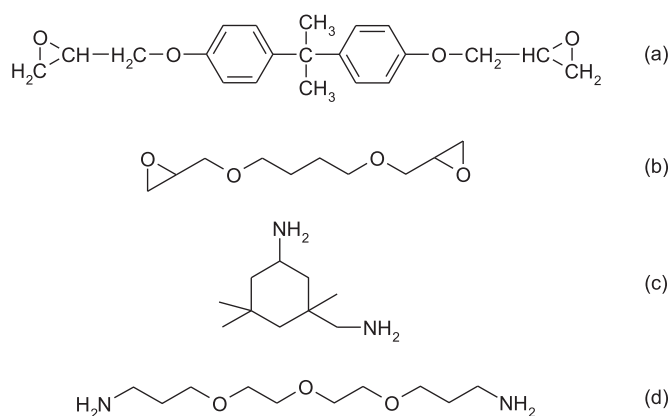


Fig. 1. Chemical structure of monomers DGEBA (a), DGEBU (b), IPDA (c), TTDA (d).

Table 1

Characteristics of the epoxy/amine networks.

Epoxy/amine system	Mass of hardener for 100 g of epoxy	Crosslink exotherm	Exotherm onset temperature	Curing cycle	Glass transition temperature
DGEBA/IPDA	25 g	563 J g^{-1} (0.47 J mol^{-1})	$80 \text{ }^\circ\text{C}$	2 h $60 \text{ }^\circ\text{C}$ in oven and post cure of 2 h in vacuum at $160 \text{ }^\circ\text{C}$	$166 \text{ }^\circ\text{C}$
DGEBU/IPDA	42 g	400 J g^{-1} (0.98 J mol^{-1})	$85 \text{ }^\circ\text{C}$	2 h $85 \text{ }^\circ\text{C}$ in oven and post cure of 3 h in vacuum at $85 \text{ }^\circ\text{C}$	$60 \text{ }^\circ\text{C}$
DGEBA/TTDA	29 g	395 J g^{-1} (0.44 J mol^{-1})	$76 \text{ }^\circ\text{C}$	1 h $60 \text{ }^\circ\text{C}$ in oven and post cure of 3 h in vacuum at $80 \text{ }^\circ\text{C}$	$69 \text{ }^\circ\text{C}$

2.2. Ageing

Thermal ageing under atmospheric air was performed in ventilated ovens (calibrated at $\pm 3 \text{ }^\circ\text{C}$) at $110 \text{ }^\circ\text{C}$ and $200 \text{ }^\circ\text{C}$.

The influence of oxygen pressure was studied by performing ageing tests in autoclaves under 50 bars of pure oxygen at $110 \text{ }^\circ\text{C}$.

2.3. Characterization

2.3.1. Oxidative products concentrations

FTIR spectroscopy in transmission mode was performed on free standing films using a Frontier spectrophotometer (PerkinElmer) in the 550 to 4000 cm^{-1} wavenumber range by averaging 16 scans with a 4 cm^{-1} resolution. Spectra were interpreted using the Spectrum software (PerkinElmer) in order to determine the absorbance value from which the concentrations in main oxidation products (carbonyls and amides) was calculated according to the method defined elsewhere [20].

2.3.2. Glass transition measurement

Differential scanning calorimetry measurements were made with a DSC Q1000 (TA Instruments). Samples with mass ranging between 3 and 5 mg sealed in aluminum pans were heated from $0 \text{ }^\circ\text{C}$ to $250 \text{ }^\circ\text{C}$ at a $10 \text{ }^\circ\text{C min}^{-1}$ ramp under nitrogen flow (50 ml min^{-1}). Results were interpreted using TA Analysis software. DSC analyses were done to check the total cure of samples and to measure the value of the glass transition temperature of aged samples. T_g values were measured during the second heating ramp (i.e. after having removed the thermal history of samples) at the inflexion point of the thermogram. Measurements were duplicated to control measurements reproducibility.

3. Results

The measurement of glass transition temperature of the networks is particularly interesting since it is related to the concentration and the flexibility of elastically active chains (those two quantities will be more precisely defined in the "Discussion" section). T_g changes after ageing under air at 110 and $200 \text{ }^\circ\text{C}$ are given in Fig. 2. It can be observed that:

- DGEBA/IPDA displays a significant T_g decrease under air, suggesting that oxidation induces an increase in the flexibility of segments and/or scissions of elastically active chains.
- DGEBA/TTDA displays a significant T_g increase under air, suggesting that oxidation induces a decrease in the flexibility of segments and/or crosslinking.
- DGEBU/IPDA shows first a slight T_g decrease but reactions responsible for an increase of T_g seem to occur at high degradation level which means that they involve whether oxidation by products or sites with a low reactivity that are « activated » by a sort of co-oxidation process.

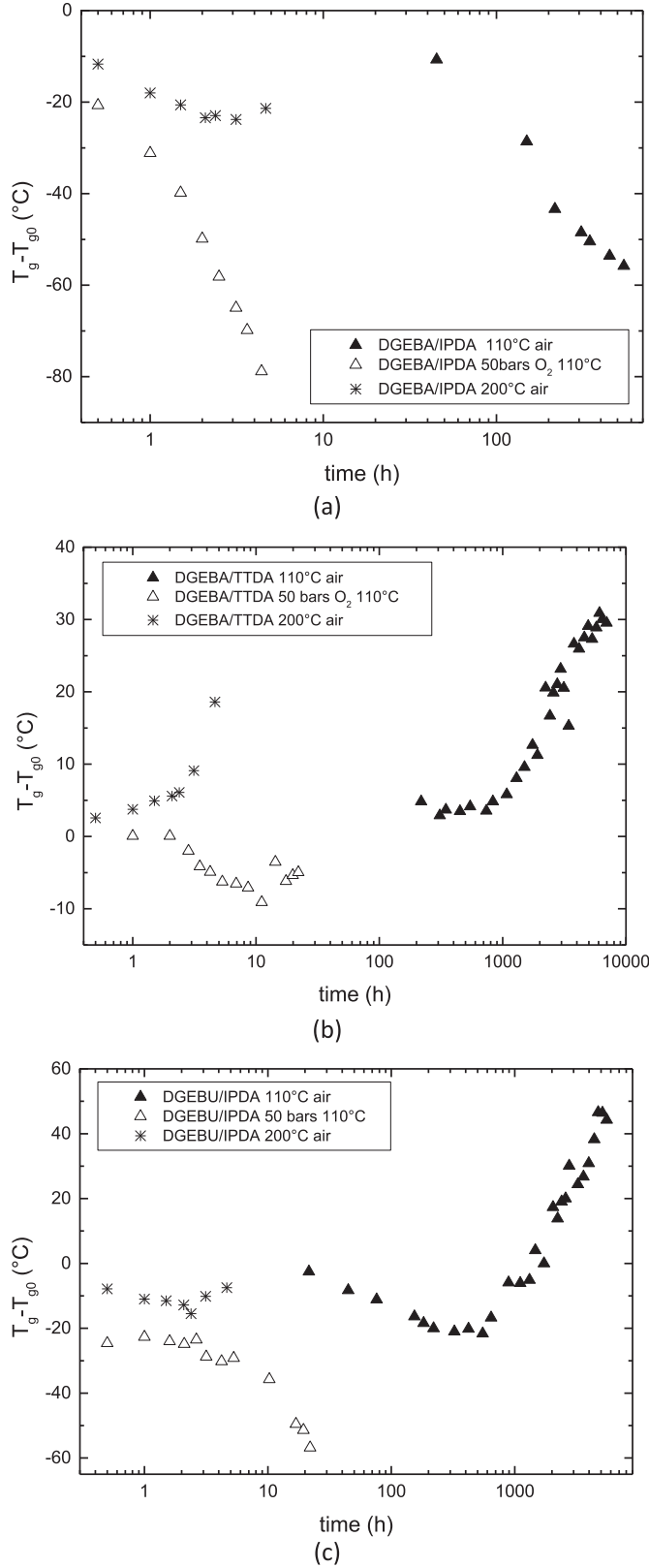


Fig. 2. T_g changes versus time for DGEBA/IPDA (a), DGEBA/TTDA (b) and DGEBU/IPDA (c).

For DGEBA/TTDA and DGEBU/IPDA, results under 50 bars O_2 indicate that reactions responsible for T_g increase are suppressed. It suggests they originate from reactions between alkyl radicals being

negligible under high oxygen pressures where terminations between POO^\bullet predominate.

It appears also that reactions responsible for T_g increase are slightly favored by temperature. On the assumption that T_g increase comes from crosslinking, this would not be surprising since this later originates from bimolecular processes that are favored at higher temperatures where macromolecular mobility is enhanced.

Last, it appears that the common point of networks displaying T_g increase (DGEBA/TTDA and DGEBU/IPDA) is the presence of methylenic sequences, which will be discussed in the following.

4. Discussion

The main aims of this section are:

- to investigate if T_g changes come from chain scissions and crosslinking of elastically active chains and/or changes in the flexibility of these segments.
- to propose a mechanistic explanation consistent with the effect of oxygen pressure.

For that purpose, we will use the DiMarzio's theory [21] in which parameters are calculated using the additive group contributions proposed by Bellenger and Verdu [22].

4.1. On the effect of structure on the initial T_g values

The glass transition of an ideal fully cured network is expected to obey DiMarzio's equation [21]:

$$T_g = \frac{T_{gl}}{1 - (K_{DM}Fn)} \quad (1)$$

Where:

- K_{DM} is the DiMarzio's constant ca 2.91 for epoxy/amine trifunctional networks [22].
- n is the crosslink density (mol kg^{-1}).
- T_{gl} is the glass transition of the corresponding « virtual » linear polymer.
- F is the Flex parameter (kg mol^{-1}) related to the molar mass per flexible bond.

T_{gl0} , F_0 and n_0 (the subscript 0 stands for virgin materials) can be assessed for unaged networks as presented in the following:

- ① T_{gl0} can be predicted from the hypothesis of additive contribution of single components:

$$T_{gl0} = \frac{M_{UCR}^*}{\sum M_i T_{gli}^{-1}} \quad (2)$$

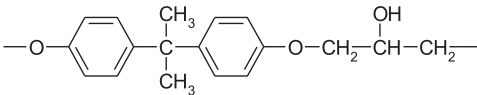


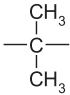

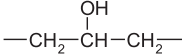
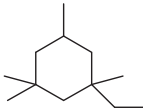
Where:

- M_{UCR}^* is the molar mass of a single repetitive unit (made of two prepolymer and a hardener unit but in which contribution of nitrogen atoms in crosslinks is suppressed).
- $M_i T_{gli}^{-1}$ is the contribution of each single component to T_{gl0} . Values are given in Table 2. The contribution for IPD cycle (not given in Ref. [22]) was estimated as follows:

① First T_{gl} of TTDA hardener was measured experimentally by DSC: $T_{gl} = 238.2 \text{ K}$. It is then possible to evaluate the contribution of the NH_2 on $M_i T_{gli}^{-1}$:

$$M_{TTDA}/(T_g)_{TTDA} = 3(M/T_g)_{-O-} + 10(M/T_g)_{-CH_2-} + 2(M/T_g)_{-NH_2}$$

Table 2Component values for T_{g10} calculation from Ref. [22] except for IPD (this work – see text).

Unit	$M \cdot T_g^{-1}$ ($\text{g mol}^{-1} \text{K}^{-1}$)	T_g (K)
	0.78	364
	0.06306	254
	0.06	233
	0.07586	554
	0.1677	453
	0.24262	239
	0.341	404.7

$$\rightarrow (M/T_g)_{\text{NH}_2} = 0.14677$$

⊙ Thanks to experimental value of T_{g1} for IPDA ($T_{g1} = 268 \text{ K}$) and contribution of NH_2 from TTDA, the contribution of IPD can be determined:

$$M_{\text{IPDA}}/(T_g)_{\text{IPDA}} = (M/T_g)_{\text{IPD}} + 2(M/T_g)_{\text{-NH}_2} = 170/268$$

$$\rightarrow (M/T_g)_{\text{IPD}} = 0.341$$

The final T_{g10} values are given in Table 3.

⊙ The Flex is defined as the ratio of molar mass of groups (without amine ends for hardener) per number of flexible bond γ (see Table 4). The values F_0 for virgin networks were then calculated using:

$$F_0 = (2 \times F_1 + F_2)/3 \quad (3)$$

F_1 and F_2 corresponding respectively to the prepolymer and the diamine hardener (TTD and IPD means that amine ends shall not to be taken into account in the calculation of flex for hardener segment) are given in Table 4 and F_0 values in Table 3.

⊙ The crosslink density n_0 was calculated as:

$$n_0 = 2/M_{\text{UCR}} \quad (4)$$

Experimental and calculated T_g values are acceptably close (Table 3). It militates in favor of using DiMarzio's approach for investigating the origin of T_g changes observed during thermal

ageing in the following of this investigation.

4.2. On the origins of glass transition changes during ageing

The aim of this section is to quantitatively discuss on the origin of T_g changes observed in Fig. 2.

As pointed out in the "Results" section for DGEBA/TTDA and DGEBU/IPDA, the reactions involving positive changes in T_g occur under air and their influence decrease when elevating the oxygen pressure. The most satisfying explanation is that those reactions are terminations involving alkyl radicals such as $\text{P}^\circ + \text{P}^\circ \rightarrow$ inactive products [23]. The consequences on T_g of such reactions will now be envisaged.

In DGEBA group, as assumed by Devanne et al. [24,25], the crosslinking between two radicals hold by 2-hydroxypropyl ether groups seems unlikely for two reasons:

- their steric hindrance,
- alkyl radicals react by β -scission (Scheme 1).

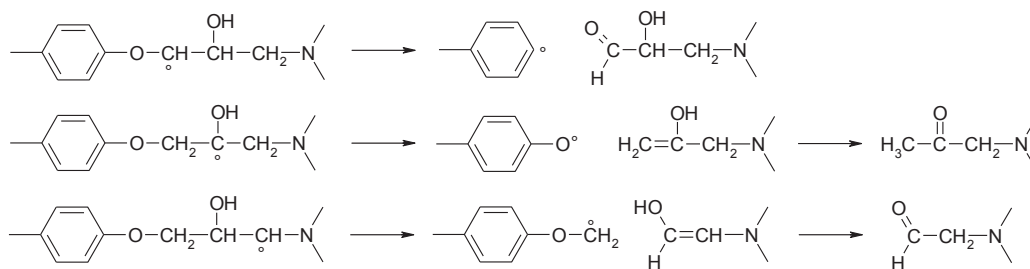
DGEBA group is thus expected to generate chain scissions rather

Table 4
Flex parameter calculation.

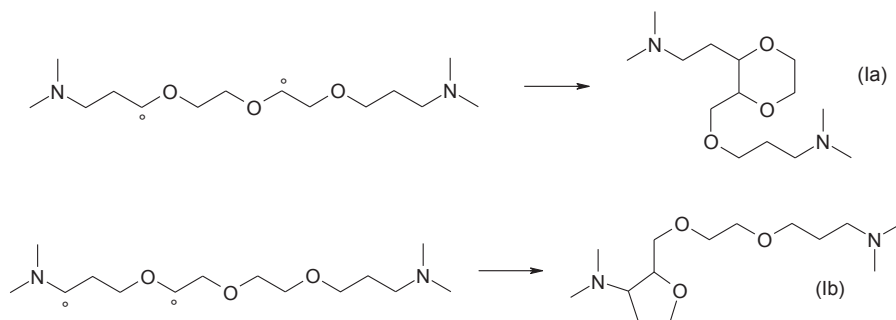
	M (g mol^{-1})	γ	F (g mol^{-1})
DGEBA	342	12	28.5
DGEBU	204	13	15.7
IPD	138	5	27.6
TTD	188	14	13.4

Table 3Calculations using Eqs. (1)–(4) of T_{g0} for each epoxy/diamine system ($T_{g0 \text{ calc}}$) and comparisons with experimental results ($T_{g0 \text{ exp}}$).

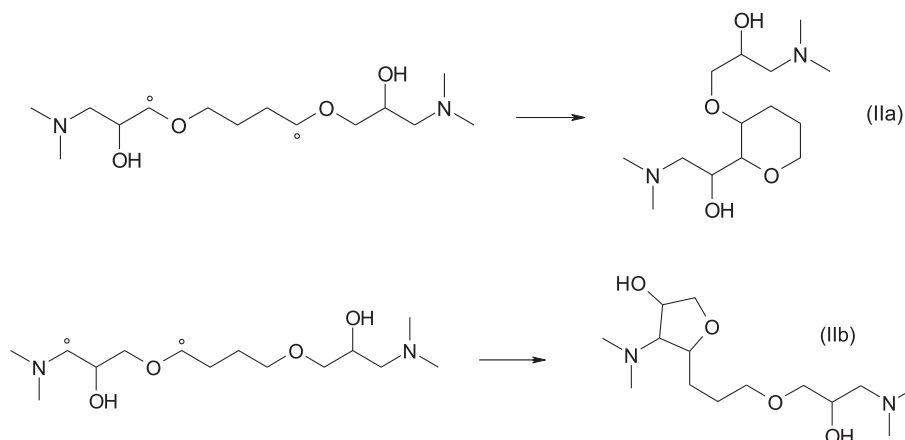
	$\sum M_i/T_{gi}$ ($\text{g mol}^{-1} \text{K}^{-1}$)	T_{g10} (K)	F_0 (g mol^{-1})	M_{UCR} (g mol^{-1})	n_0 (mol kg^{-1})	$T_{g0 \text{ exp}}$ (K)	$T_{g0 \text{ calc}}$ (K)
DGEBA/TTDA	2.834	307.6	23.5	900	2.35	343	363
DGEBA/IPDA	2.386	344.5	28.2	850	2.22	439	427
DGEBU/IPDA	2.044	264.2	19.7	572	3.5	333	330



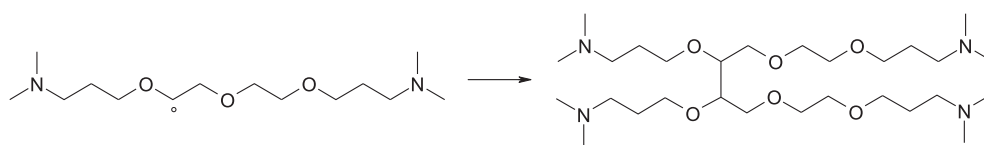
Scheme 1. Possible degradation pathway of alkyl radicals in DGEBA.



Scheme 2. Possible intramolecular termination processes in TTDA group.



Scheme 3. Possible intramolecular termination processes in DGEBU group.



Scheme 4. Possible mechanisms for crosslinking involving TTDA group.

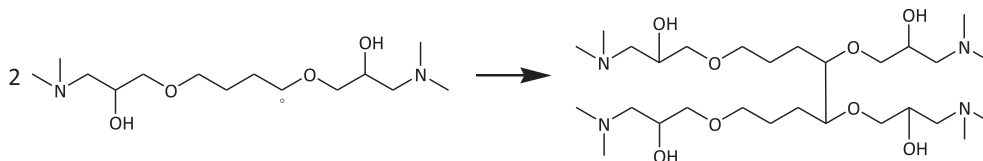
than crosslinking either under inert (Scheme 1) or oxygenated atmosphere (see later). It seems also difficult to envisage that two alkyl radicals held by IPDA groups react to give a crosslink, here also due to the steric hindrance of substituted aliphatic rings [20]. The T_g increase observed in DGEBA/TTDA and DGEBU/IPDA is hence expected to come from reactions occurring in TTDA or DGEBU units.

If radicals are created in α position of heteroatoms in TTDA or DGEBU (which is consistent with the nature of stable products observed in FTIR [20]), various intramolecular coupling processes

(cyclization) lead to 5 or 6 members rings and a subsequent increase of T_{g1} and Flex parameters (Schemes 2 and 3) or crosslinking between chains (Schemes 4 and 5).

According to Eq. (1), those reactions could be interpreted as changes in:

- concentration of elastically active chain i.e. crosslink density (n),
- flex parameter (F),
- glass transition temperature of the linear polymer (T_{g1}).



Scheme 5. Possible mechanisms for crosslinking involving DGEBU group.

Table 5

Calculation of T_g changes in case of intramolecular termination of radicals (see Schemes 2–7) and comparison with experimental changes. Here, M^* , the number of rotatable bonds γ^* and flex F^* stands for the group being modified by oxidation, F_{aged} comes from Eq. (3) using F^* and $\Delta F = F_{aged} - F_0$ (F_0 given in Table 3).

	M^* (g mol ⁻¹)	γ^*	F^* (g mol ⁻¹)	F_{aged} (g mol ⁻¹)	ΔF (g mol ⁻¹)	ΔT_g with $T_{g0} = 307.6$ K, $n_0 = 2.35$ mol kg ⁻¹
TTDA → Ia	186	10	18.6	25.2	1.7	+14 K (+30 K experimentally observed)
TTDA → Ib	186	11	16.9	24.6	1.1	+18 K (+30 K experimentally observed)
	M^* (g mol ⁻¹)	γ^*	F^* (g mol ⁻¹)	F_{aged} (g mol ⁻¹)	ΔF (g mol ⁻¹)	ΔT_g with $T_{g0} = 264.2$ K, $n_0 = 3.50$ mol kg ⁻¹
DGEBU → IIa	182	9	20.2	22.7	3	+27 K (+40 K experimentally observed)
DGEBU → IIb	182	10	18.2	21.3	1.6	+24 K (+40 K experimentally observed)
	M^* (g mol ⁻¹)	γ^*	F^* (g mol ⁻¹)	F_{aged} (g mol ⁻¹)	ΔF (g mol ⁻¹)	ΔT_g with $T_{g0} = 344.5$ K, $n_0 = 2.22$ mol kg ⁻¹
IPDA → III	153	7	21.9	26.3	-1.9	-16 K (-60 K experimentally observed)

We will now discuss if the products generated by alkyl radicals coupling are consistent with experimental T_g increase using DiMarzio's equation as a "filter".

Reactions leading to a change in Flex parameter (e.g. intramolecular cyclization) are also expected to change the value of T_{gl} . It can thus be written:

$$\frac{\partial T_g}{\partial F} = \frac{\partial T_{gl}}{\partial F} \times \frac{1}{1 - K_{DM} \cdot F \cdot n_0} + \frac{T_{gl} \cdot K_{DM} \cdot n_0}{(1 - K_{DM} \cdot F \cdot n_0)^2} \quad (5)$$

Which can be rearranged using Eq. (1):

$$\frac{\partial T_g}{\partial F} = \frac{T_g}{T_{gl}} \times \left[\frac{\partial T_{gl}}{\partial F} + T_{g0} \cdot K_{DM} \cdot n_0 \right] \quad (6)$$

And finally:

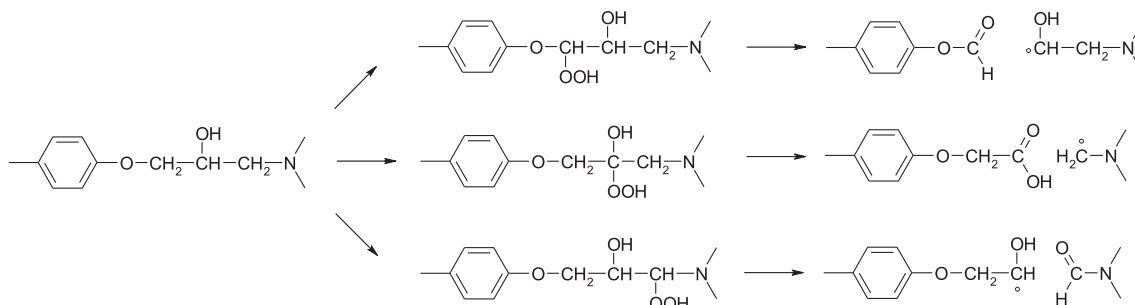
$$\Delta T_g \sim \frac{T_{g0}}{T_{gl}} \times \left[\frac{\partial T_{gl}}{\partial F} + T_{g0} \cdot K_{DM} \cdot n_0 \right] \Delta F \quad (7)$$

T_{g0} , T_{gl0} , n_0 standing for a virgin material and ΔF being the increase in Flex coming from oxidation reactions.

It can be observed in the literature, within the family of virgin epoxy/diamine (Table 5 in Ref. [22]), that:

$$\frac{\partial T_{gl}}{\partial F} \sim 4 \text{ K mol g}^{-1}$$

By combining this last relationship and Eq. (7), it is now possible



Scheme 6. Possible mechanism for chain scission in DGEBA group.

to assess T_g changes as a function of Flex changes.

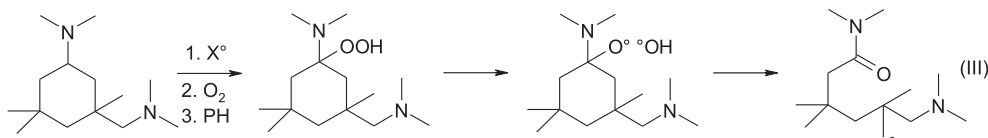
The T_g values can be recalculated using Eq. (7) in the case of 100% conversion of TTDA or DGEBU groups into cyclic by-products presented in Schemes 2 and 3. It can be shown in Table 5 that the corresponding T_g increase is lower than experimentally observed, meaning that even if those intramolecular processes are possible, they cannot quantitatively explain the experimental strong changes in T_g . The most possible reason is therefore the intermolecular reactions presented in Schemes 4 and 5.

The case of IPDA groups remains open. T_g decrease in DGEBA/IPDA and in DGEBU/IPDA might originate, at least in part, from scissions in hydroxypropyl ether groups in DGEBA and DGEBU (see Scheme 6) but the nature of degradation products of IPDA group is open. Two scenarii are possible.

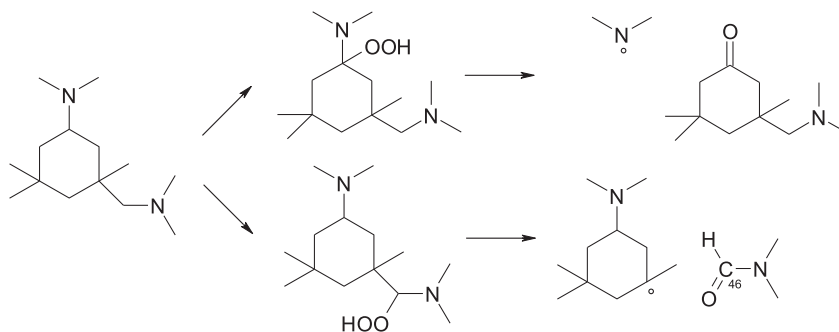
- the first induces an opening of the ring, i.e. mainly a decrease in the Flex parameter (Scheme 7). According to Table 5, this process induces only a very low decrease in final T_g value.
- the second (Scheme 8) involves the scission of an elastically active chain i.e. a decrease of the n_0 parameter in Eq. (1). It might thus be considered in complement of scissions of hydroxypropyl ether groups presented in Scheme 6.

Finally, one would have:

- for DGEBA/IPDA network: chain scissions in DGEBA and maybe IPDA groups.



Scheme 7. Possible chain scission process in IPDA group.



Scheme 8. Possible mechanism for chain scission in IPDA group.

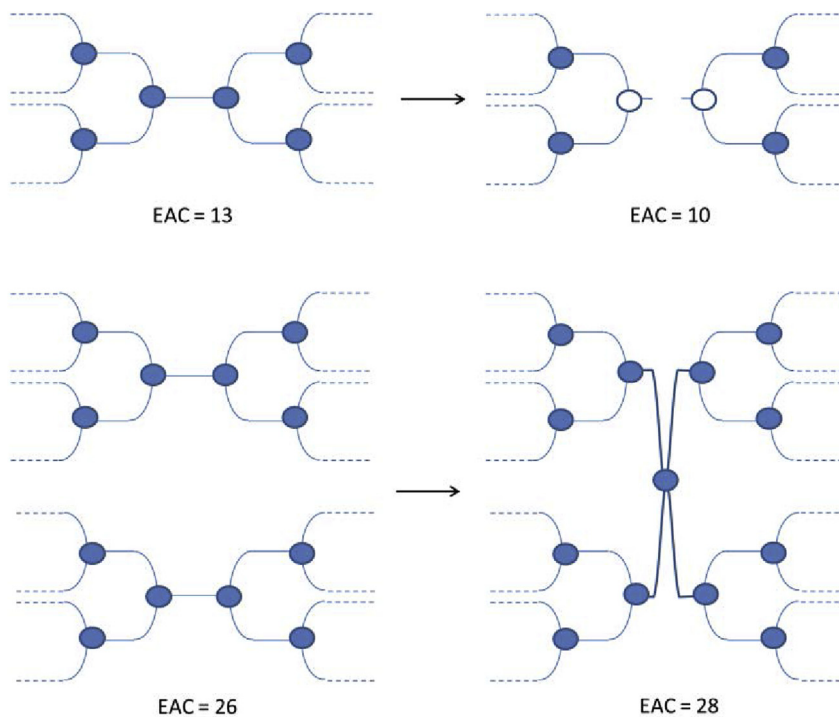


Fig. 3. Effect of chain scission or crosslinking on the number of elastically active chains. Full dots represent crosslink nodes contributing to elasticity.

- for DGEBA/TTDA network: chain scissions in DGEBA counterbalanced by crosslinking in TTDA at least under air and progressively suppressed when increasing the oxygen concentration.
- for DGEBU/IPDA network: chain scissions in hydroxypropyl ether group of DGEBU and maybe IPDA counterbalanced by crosslinking in DGEBU at least under air and progressively suppressed when increasing the oxygen concentration.

The last step of this work is to quantify those phenomena using a modification of DiMarzio's equation as presented in the next paragraph.

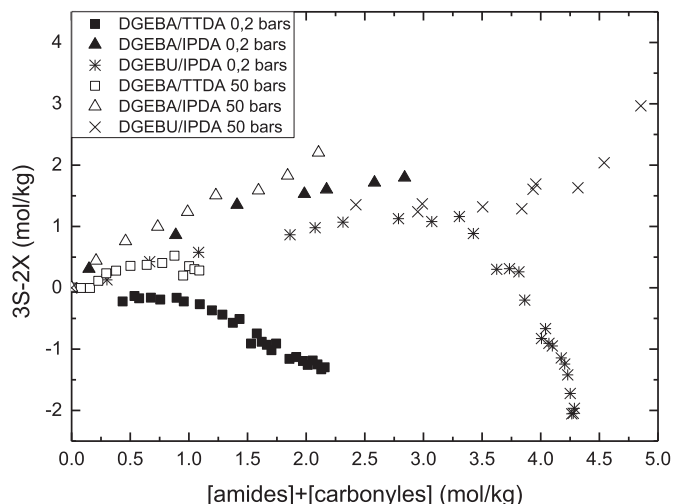
4.3. On the concentration in chain scissions and crosslinks

According to which precedes, it is clear that oxidative ageing of epoxy resins leads to chain scissions or crosslinking modifying the crosslink density such as illustrated in Fig. 3.

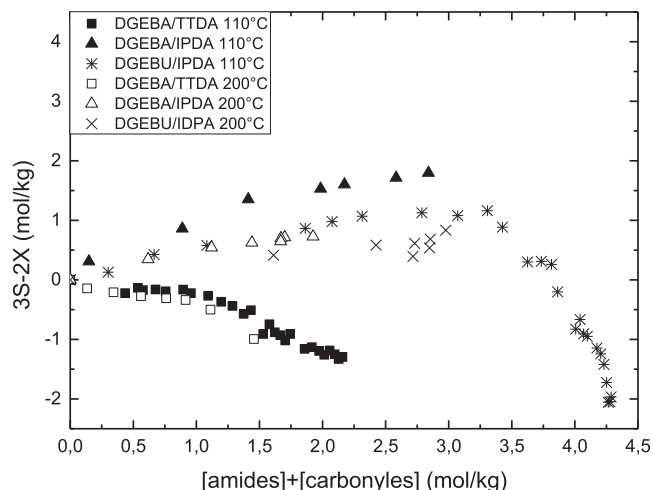
Let us recall that an elastically active (EAC) chain has its two ends that are crosslink nodes connected to the network. It can thus be shown that, at low conversion degrees (where the network is close to ideality) [26]:

In the case of exclusive chain scissions:

$$[EAC] = [EAC]_0 - 3S \quad (8)$$



(a)



(b)

Fig. 4. Changes in $3S - 2X$ versus the concentration in stable oxidation products at $110\text{ }^{\circ}\text{C}$ under air and under 50 bars O_2 (a) and under air at 110 and $200\text{ }^{\circ}\text{C}$ (b).

(S being the concentration in chain scission).

In the case of exclusive crosslink

$$[\text{EAC}] = [\text{EAC}]_0 + 2X \quad (9)$$

(X being concentration in crosslink).

And, in any case:

$$[\text{EAC}] = [\text{EAC}]_0 - 3S + 2X \quad (10)$$

For an ideal network of functionality f and crosslink density n_0 , the concentration in elastically active chains (i.e. chains ended by two crosslink nodes connected to the network) is given by:

$$[\text{EAC}]_0 = f \times n_0/2 \quad (11)$$

The DiMarzio's equation can thus be modified to express the changes in T_g in function of changes in network architecture:

$$\left(\frac{1}{T_g(t)} - \frac{1}{T_{g0}} \right) \times \frac{3T_g l}{2K_{DM} F} = 3S - 2X \quad (12)$$

The quantity $3S - 2X$ was thus plotted versus the concentration in the main oxidation products as determined in Ref. [17] in Fig. 4, so as to discuss on the occurrence of chain scission and crosslinking at a given degradation level.

It was tried, for a given system, to estimate:

- the concentration chain scission per concentration oxidation products (amides + carbonyls) from measurements under elevated oxygen pressure where crosslinking are inhibited:

$$A = 3S - 2X \sim 3S \quad (13)$$

i.e.

$$S = A/3 \quad (14)$$

where A is the slope of $3S - 2X$ vs [amides + carbonyls] under 50 bars O_2

- and then the concentration in crosslinking from the measurements under air:

$$X = (A - B)/2 \quad (15)$$

where B is the slope of $3S - 2X$ vs [amides + carbonyls] under air. Results are given in Table 6 and call for following comments:

- It is easy to see that the crosslinking is favored with the concentration in methylenic structures participating to mechanisms such as proposed in Fig. 3.
- Since accelerated ageing tests often require higher temperatures and oxygen pressures [1–3], those observations confirm the difficulty to correlate results of accelerated tests with natural ageing ones. Kinetic modeling offers a solution provided that the reactions inducing crosslinking or chains scissions are ruled by rate constants obeying Arrhenius law, and that they are used in a kinetic model describing the relative occurrence of reactions with oxygen concentration [23].

Table 6

Chain scission and crosslinking concentration (per mole of carbonyls + amides formed) calculated from Eq. (14) and Eq. (15) under several temperatures and oxygen pressures conditions.

	110 °C - 50 bar O ₂		110 °C - air		200 °C - air	
	3S - 2X ~ 3S	S	3S - 2X	X	3S - 2X	
DGEBA/IPDA	1.16	0.387	1.1	0.03	0.58	
DGEBA/TTDA	1.36	0.453	-0.19	0.78	-0.26	[CO + amides] < 1 mol kg ⁻¹
			-1.3	1.33	-1.3	[CO + amides] > 1 mol kg ⁻¹
DGEBU/IPDA	0.46	0.153	0.6	-0.07	-4.58	[CO + amides] < 2 mol kg ⁻¹
			-5	2.73		[CO + amides] > 3 mol kg ⁻¹

5. Conclusions

This paper presents a study of the thermo-oxidative ageing of three epoxy networks: DGEBA/IPDA, DGEBA/TTDA, DGEBU/IPDA, the two latter displaying some aliphatic linear sequences. Measurements of glass transition temperature (expressing the crosslink density) were derived to obtain the concentration in chain scissions and crosslinking. Those results indicate that DGEBA/TTDA and DGEBU/TTDA undergo a significant crosslinking possibly associated to the methylenic sequences. Those phenomena are partially suppressed by elevating the oxygen pressure. As a result, accelerated ageing tests using high oxygen pressures leads to complete different macromolecular modification for ageing under atmospheric conditions for a given oxidation state. Furthermore, the occurrence of crosslinking seems also possible for linear aliphatic epoxies and noticeable the new class of biobased epoxies [27,28]. In any case, it means that despite a certain commonality in changes observed by FTIR, the consequences of oxidation on backbone architecture differ for rigid or flexible epoxy resins. The consequences of either chain scissions and/or crosslinking on mechanical behavior of networks [29,30] remains to be investigated in the case of epoxies.

Acknowledgements

ANRT (CIFRE N°2013/0356) is gratefully acknowledged for financial support.

References

- [1] N. Rasoldier, X. Colin, J. Verdu, M. Bocquet, L. Olivier, L. Chocinski-Arnault, M.C. Lafarie-Frenot, Model systems for thermo-oxidised epoxy composite matrices, *Compos. Part A Appl. Sci. Manuf.* 39 (Issue 9) (September 2008) 1522–1529.
- [2] M. Pecora, Y. Pannier, M.-C. Lafarie-Frenot, M. Gigliotti, C. Guigon, Effect of thermo-oxidation on the failure properties of an epoxy resin, *Polym. Test.* 52 (July 2016) 209–217.
- [3] M. Minervino, M. Gigliotti, M.C. Lafarie-Frenot, J.C. Grandidier, The effect of thermo-oxidation on the mechanical behaviour of polymer epoxy materials, *Polym. Test.* 32 (Issue 6) (September 2013) 1020–1028.
- [4] C. Damian, E. Espuche, M. Escoubes, Influence of three ageing types (thermal oxidation, radiochemical and hydrolytic ageing) on the structure and gas transport properties of epoxy-amine networks, *Polym. Degrad. Stab.* 72 (Issue 3) (June 2001) 447–458.
- [5] L. Olivier, N.Q. Ho, J.C. Grandidier, M.C. Lafarie-Frenot, Characterization by ultra-micro indentation of an oxidized epoxy polymer: correlation with the predictions of a kinetic model of oxidation, *Polym. Degrad. Stab.* 93 (Issue 2) (February 2008) 489–497.
- [6] X. Buch, M.E.R. Shanahan, Thermal and thermo-oxidative ageing of an epoxy adhesive, *Polym. Degrad. Stab.* 68 (Issue 3, 11) (May 2000) 403–411.
- [7] J. Decelle, N. Huet, V. Bellenger, Oxidation induced shrinkage for thermally aged epoxy networks, *Polym. Degrad. Stab.* 81 (Issue 2) (2003) 239–248.
- [8] X. Colin, C. Marais, J. Verdu, Kinetic modelling and simulation of gravimetric curves: application to the oxidation of bismaleimide and epoxy resins, *Polym. Degrad. Stab.* 78 (Issue 3) (2002) 545–553.
- [9] M.C. Lafarie-Frenot, S. Rouquié, N.Q. Ho, V. Bellenger, Comparison of damage development in C/epoxy laminates during isothermal ageing or thermal cycling, *Compos. Part A Appl. Sci. Manuf.* 37 (Issue 4) (April 2006) 662–671.
- [10] B.J. Anderson, Thermal stability of high temperature epoxy adhesives by thermogravimetric and adhesive strength measurements, *Polym. Degrad. Stab.* 96 (Issue 10) (October 2011) 1874–1881.
- [11] B.J. Anderson, Thermal stability and lifetime estimates of a high temperature epoxy by Tg reduction, *Polym. Degrad. Stab.* 98 (Issue 11) (November 2013) 2375–2382.
- [12] F. Daghia, F. Zhang, C. Cluzel, P. Ladevèze, Thermo-mechano-oxidative behavior at the ply's scale: the effect of oxidation on transverse cracking in carbon-epoxy composites, *Compos. Struct.* 134 (15) (December 2015) 602–612.
- [13] S. Terekhina, M. Mille, B. Fayolle, X. Colin, Oxidation induced changes in viscoelastic properties of a thermally stable epoxy matrix, *Polym. Sci. Ser. A* 55 (Issue 10) (October 2013) 614–624.
- [14] E.T. Denisov, I.B. Afanas'ev, *Oxidation and Antioxidants in Organic Chemistry and Biology*, CRC Press, March 29, 2005.
- [15] J. Decelle, N. Huet, V. Bellenger, Oxidation induced shrinkage for thermally aged epoxy networks, *Polym. Degrad. Stab.* 81 (Issue 2) (2003) 239–248.
- [16] M.C. Lafarie-Frenot, S. Rouquié, N.Q. Ho, V. Bellenger, Comparison of damage development in C/epoxy laminates during isothermal ageing or thermal cycling, *Compos. Part A Appl. Sci. Manuf.* 37 (Issue 4) (April 2006) 662–671.
- [17] V. Bellenger, J. Verdu, Oxidative skeleton breaking in epoxy-amine networks, *J. Appl. Polym. Sci.* 30 (Issue 1) (1985) 363–374.
- [18] C. Galant, B. Fayolle, M. Kuntz, J. Verdu, Thermal and radio-oxidation of epoxy coatings, *Prog. Org. Coatings* 69 (Issue 4) (December 2010) 322–329.
- [19] Y. Zahra, F. Djouani, B. Fayolle, M. Kuntz, J. Verdu, Thermo-oxidative aging of epoxy coating systems, *Prog. Org. Coatings* 77 (Issue 2) (February 2014) 380–387.
- [20] E. Ernault, E. Richaud, B. Fayolle, Thermal oxidation of epoxies: influence of diamine hardener, *Polym. Degrad. Stab.* 134 (December 2016) 76–86.
- [21] E.A. DiMarzio, On the second-order transition of a rubber, *J. Res. Natl. Bureau Stand. Sect. A Phys. Chem.* 68 (1964) 611–617.
- [22] V. Bellenger, J. Verdu, E. Morel, Effect of structure on glass transition temperature of amine crosslinked epoxies, *J. Polym. Sci. Part B Polym. Phys.* 25 (Issue 6) (June 1987) 1219–1234.
- [23] E. Richaud, F. Farcas, P. Bartoloméo, B. Fayolle, L. Audouin, J. Verdu, Effect of oxygen pressure on the oxidation kinetics of unstabilised polypropylene, *Polym. Degrad. Stab.* 91 (Issue 2) (February 2006) 398–405.
- [24] T. Devanne, A. Bry, L. Audouin, J. Verdu, Radiochemical ageing of an amine cured epoxy network. Part I: change of physical properties, *Polymer* 46 (Issue 1, 6) (January 2005) 229–236.
- [25] T. Devanne, A. Bry, N. Raguin, M. Sebban, P. Palmas, L. Audouin, J. Verdu, Radiochemical ageing of an amine cured epoxy network. Part II: kinetic modelling, *Polymer* 46 (Issue 1, 6) (January 2005) 237–241.
- [26] E. Richaud, P. Gilormini, M. Coquillat, J. Verdu, Crosslink density changes during the hydrolysis of tridimensional polyesters, *Macromol. Theory Simulations* 23 (Issue 5) (June 2014) 320–330.
- [27] E. Darroman, N. Durand, B. Boutevin, S. Caillol, New cardanol/sucrose epoxy blends for biobased coatings, *Prog. Org. Coatings* 83 (June 2015) 47–54.
- [28] R. Auvergne, S. Caillol, G. David, B. Boutevin, J.-P. Pascault, Biobased thermosetting epoxy: present and future, *Chem. Rev.* 114 (Issue 2) (2014) 1082–1115.
- [29] J.E. Martin, D. Adolf, Constitutive equation for cure-induced stresses in a viscoelastic material, *Macromolecules* 23 (Issue 23, 1) (January 1990) 5014–5019.
- [30] P.Y. Le Gac, D. Choqueuse, M. Paris, G. Recher, C. Zimmer, D. Melot, Durability of polydicyclopentadiene under high temperature, high pressure and seawater (offshore oil production conditions), *Polym. Degrad. Stab.* 98 (Issue 3) (March 2013) 809–817.